Wicking in Porous Materials

Traditional and Modern Modeling Approaches

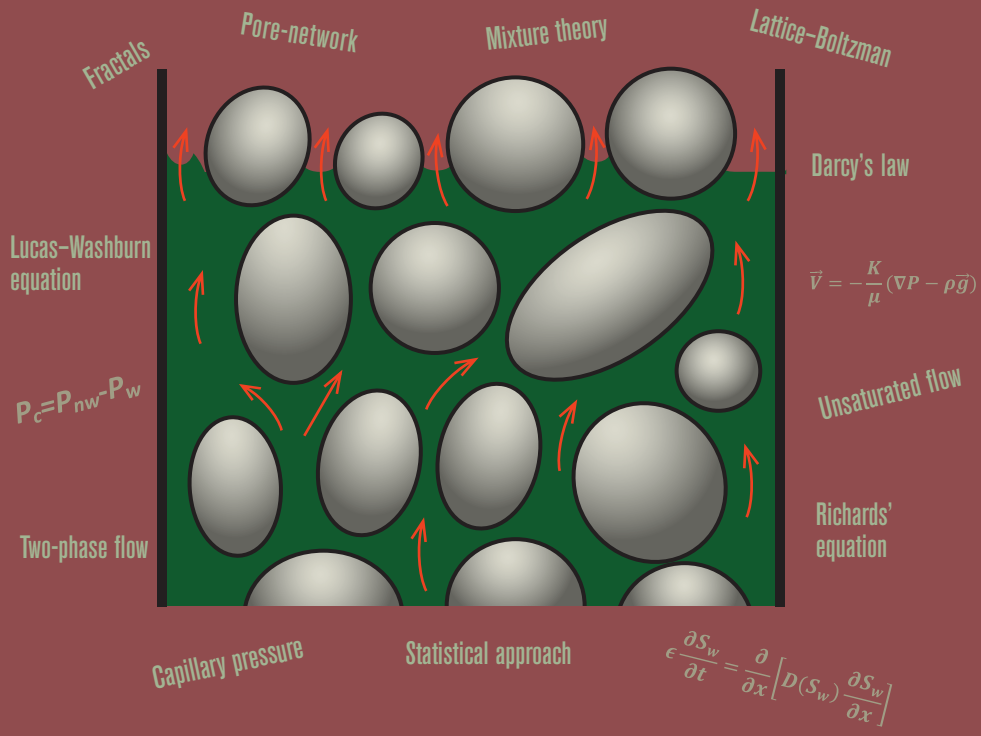

Edited by

Reza Masoodi

Krishna M. Pillai

CRC Press
Taylor & Francis Group

Wicking in Porous Materials

Traditional and Modern Modeling Approaches

Wicking in Porous Materials

Traditional and Modern Modeling Approaches

Edited by

Reza Masoodi

Krishna M. Pillai

CRC Press
Taylor & Francis Group
Boca Raton London New York

CRC Press is an imprint of the
Taylor & Francis Group, an **informa** business

CRC Press
Taylor & Francis Group
6000 Broken Sound Parkway NW, Suite 300
Boca Raton, FL 33487-2742

Version Date: 2012920

International Standard Book Number-13: 978-1-4398-7433-2 (eBook - PDF)

Contents

Preface

Wicking or spontaneous imbibition of liquids into dry porous media is an industrial problem of great relevance—it finds application in a range of fields from textile processing to food processing to the processing of composite materials. A leading consumer product company funded our research on the wicking performance of one of their products over the last decade. These series of projects brought us to the amazing world of wicking and absorbent technology. While working in this area and conducting an exhaustive literature survey, we realized that different mathematical models based on varied flow physics are available for modeling liquid flow in porous materials during wicking. However, there was no book or publication that could present *all* the different modeling approaches in one volume in order to compare and disseminate the varied approaches. Hence, in 2010, we decided to collect these approaches and present them in the form of a book such that the basic assumptions and mathematical details associated with each of these methodologies are described. This project required about 2 years of hard work to accomplish our dream and publish this book.

The book contains some of the most important methods and philosophies for modeling wicking, from the traditional models to the latest approaches developed during the last few years. Although we tried to be as inclusive as possible, some important developments in the field may have escaped our dragnet. For example, application of the Ising model to predict the migration of moisture in a network of fibers could not be included due to a lack of contributing authors in the area. Similarly, the statistical approach to model wicking after accounting for randomness in porous media could not be included due to a shortage of time. Despite these shortcomings, we hope this book will be useful to our intended users. Although we have tried to be as meticulous and exact as possible in our work, some mistakes and oversights might have slipped in—we apologize for these misses.

In general, the book is intended for graduate students, professors, scientists, and engineers who are engaged in research and development on wicking and absorbency. In particular, the book is aimed at mathematical modelers who want to predict wicking with the help of computer programs—our goal is to provide a sound conceptual framework for learning the science behind different mathematical models, while at the same time being aware of the practical issues of model validation as well as measurement of important properties and parameters associated with various models. The layout of the book is designed to help in this task. Chapter 1 begins with an introduction on wicking, while Chapter 2 introduces the science behind wetting of surfaces. Chapter 3 introduces the reader to the basic derivation of the capillary model, and extension of the model after including gravity,

inertia, and other effects. Since many of the recent models treat wicking as a flow-in-porous-media-type problem, Chapter 4 is dedicated to the science of single- and multi-phase flows in porous media, followed by a brief description of the measurement techniques and theoretical models available for the associated porous-media properties. The remaining chapters provide details of the individual models developed for wicking. Chapter 5 describes how the single-phase flow model accompanied by a sharp-front approximation is effective in modeling liquid imbibition into porous wicks. Chapter 6 describes the application of the unsaturated-flow (Richard's equation) model to predict wicking in anisotropic fibrous media. Chapter 7 discusses the application of the same unsaturated flow approach to model wicking-type liquid movements in absorbent swelling porous materials. Chapter 8 presents an application of the network models to model wicking accompanied by evaporation in porous materials. Chapter 9 explains advanced two-phase flow physics in network models used to study microscopic aspects of the wicking phenomenon. Chapter 10 describes a fractal-based approach to model wicking in porous media. In Chapter 11, wicking in deformable sponge is predicted after using the mixture theory to set up the governing equations. Finally, the use of the Lattice Boltzmann method to conduct a direct numerical simulation of wicking flows is presented in Chapter 12.

Our special thanks go to the individual authors who contributed chapters in this book—this project would not have been possible without their hardwork, support, and faith in this project. We are sure they will share our happiness and pride in publishing this book. We would like to express our appreciation to CRC Press for providing us with an opportunity to bring this work to fruition. In particular, we would like to thank the resourceful Jonathan Plant, executive editor at CRC Press, who encouraged and helped us at all stages of the project while doing a bit of firefighting for us to keep the project on track. We also thank Amber Donley, project coordinator at CRC Press, for her help. We also thank Syed Mohamad Shajahan, project manager at Techset Composition who oversaw the production of this book. A special thanks is reserved for Michelle Schoenecker and Dr. Marjorie Piechowski for helping us with the editing of our own chapters. We would also like to acknowledge Milad Masoodi's help in designing the book cover. Finally, we take this opportunity to express our deep appreciation to our families for their understanding and support during the course of this project that required many hours of activity during holidays, evenings, and weekends.

Reza Masoodi
Philadelphia, Pennsylvania

Krishna M. Pillai
Milwaukee, Wisconsin

Editors

Dr. Reza Masoodi is an assistant professor at Philadelphia University. He holds a PhD in mechanical engineering from the University of Wisconsin-Milwaukee (UWM). His PhD dissertation was about modeling imbibition of liquids into rigid and swelling porous media. His research areas of interests are flow in porous media, convection heat transfer, CFD, nano-composites, heat exchangers, and renewable energy. Dr. Masoodi has completed several research projects on single-phase flow in rigid and swelling porous media, capillary pressure, and permeability changes due to swelling. He has published several research papers, technical reports, and book chapters in the area of wicking in porous media. Dr. Masoodi is also a reviewer for more than 20 journals and served as technical committee member or peer reviewer for several scientific conferences.

Dr. Krishna M. Pillai is an associate professor at University of Wisconsin-Milwaukee (UWM) and is also the director of Laboratory for Flow and Transport Studies in Porous Media at UWM. He holds a BTech and MTech from IIT Kanpur (India), PhD from the University of Delaware, and post-doctoral fellowship at the University of Illinois, Urbana-Champaign. His research interests lie in several areas of porous media transport including flow and transport in fibrous media, wicking in rigid and swelling porous media, processing of polymer–matrix and metal–matrix composites, and evaporation modeling using network and continuum models. He has published extensively in reputed journals and presented his work in numerous international conferences and workshops. He is also a coauthor of several book chapters. He received copyright protections (sponsored by UWM Research Foundation) for his simulation codes PORE-FLOW and MIMPS. He was awarded the prestigious CAREER grant in 2004 by the National Science Foundation of the United States to model and simulate flow processes during mold filling in liquid molding processes used for manufacturing polymer composites. During his sabbatical in 2007–2008, he was a visiting researcher at CNRS at Institut de Mécanique des Fluides de Toulouse, France.

Contributors

Daniel M. Anderson
Department of Mathematical Sciences
George Mason University
Fairfax, Virginia

Holger Beruda
Procter&Gamble Service GmbH
Schwalbach am Taunus, Germany

Thomas M. Bucher
Department of Mechanical and Nuclear Engineering
Virginia Commonwealth University
Richmond, Virginia

Jianchao Cai
Institute of Geophysics and Geomatics
China University of Geosciences
Wuhan, People's Republic of China

Volker Clausnitzer
Groundwater Modeling Centre
DHI-Wasy GmbH
Berlin, Germany

Hans-Jörg G. Diersch
Groundwater Modeling Centre
DHI-Wasy GmbH
Berlin, Germany

Sandrine Geoffroy
Institut Clément Ader
Université de Toulouse
Toulouse, France

S. Majid Hassanizadeh
Department of Earth Sciences
Utrecht University
Utrecht, the Netherlands

Kamel Hooman
School of Mechanical and Mining Engineering
The University of Queensland
Queensland, Australia

Xiangyun Hu
Institute of Geophysics and Geomatics
China University of Geosciences
Wuhan, People's Republic of China

Vahid Joekar-Niasar
Innovation and R&D Department
Shell Global Solutions International
Rijswijk, the Netherlands

Manuel Marcoux
Institut de Mécanique des Fluides de Toulouse
Université de Toulouse
and
CNRS
Toulouse, France

Reza Masoodi
School of Design and Engineering
Philadelphia University
Philadelphia, Pennsylvania

Vladimir Mirnyy
Groundwater Modeling Centre
DHI-Wasy GmbH
Berlin, Germany

Krishna M. Pillai
Department of Mechanical Engineering
University of Wisconsin—Milwaukee
Milwaukee, Wisconsin

Mark L. Porter
Earth and Environmental Sciences (EES-14)
Los Alamos National Laboratory
Los Alamos, New Mexico

Marc Prat
Institut de Mécanique des Fluides de Toulouse
Université de Toulouse
and
CNRS
Toulouse, France

Rodrigo Rosati
Procter & Gamble Service GmbH
Schwalbach am Taunus, Germany

Marcel G. Schaap
Department of Soil, Water and Environmental Science
The University of Arizona
Tucson, Arizona

Mattias Schmidt
Procter & Gamble Service GmbH
Schwalbach am Taunus, Germany

Javed I. Siddique
Department of Mathematics
Pennsylvania State University
York, Pennsylvania

Hooman Vahedi Tafreshi
Department of Mechanical and Nuclear Engineering
Virginia Commonwealth University
Richmond, Virginia

Stéphanie Veran-Tissoires
Institut de Mécanique des Fluides de Toulouse
Université de Toulouse
and
CNRS
Toulouse, France

Boming Yu
School of Physics
Huazhong University of Science and Technology
Wuhan, People's Republic of China

Jijie Zhou
Shanghai Institute of Applied Mathematics and Mechanics
Shanghai University
Shanghai, People's Republic of China

1

Introduction to Wicking in Porous Media

Reza Masoodi and Krishna M. Pillai

CONTENTS

Wicking or spontaneous imbibition is the suction of a liquid into a porous medium due to the negative capillary pressure created at the liquid–air interfaces. The capillary pressure arises as a result of wetting the surface of the solid particles by the invading liquid that causes a change in the surface energy of the solid phase. In this chapter, an estimation of the capillary pressure through the Young–Laplace equation is presented, and the capillary and hydraulic radii, important parameters in the equation, are discussed. Some important applications of wicking in industry as well as in nature are briefly discussed next. Finally, an overview is presented of the different modeling approaches possible for wicking, which include the traditional capillary models, the porous-continuum models, the discrete models, and the statistical approaches.

1.1 Introduction

Imbibition is defined as the displacement of one fluid by another fluid, immiscible and more viscous than the first, in a porous medium (Alava et al., 2004). Examples of imbibition are displacement of oil by another immiscible liquid during oil recovery (Sorbie et al., 1995), invasion of a dry fiber-preform by a resin in resin transfer molding (Pillai, 2004), penetration of ink into paper (Schoelkopf, 2002), and movement of a liquid into a porous surface during the wiping-off of the liquid from the surface (Lockington and Parlange, 2003). If the driving force that causes imbibition is the capillary pressure, then such an imbibition is called wicking (also known as capillarity) (Masoodi et al., 2007). In other words, *wicking is the spontaneous imbibition of a liquid into a porous substance due to the action of capillary pressure*. Wicking may also occur from a combination of capillary pressure and an external pressure (Masoodi et al., 2010). Wicking plays an important role in many phenomena observed in science, industry, and everyday life. For example, in heat pipes, nano- and micro-wicks, wipes, sponges, diapers, and feminine pads, the wicking capability of the porous material involved is of high importance. Wicking also happens in nature; for example, in green plants, both capillary and osmotic pressures are responsible for drawing water and minerals from the roots up to the leaves (Ksenzhek and Volkov, 1998).

There are two proven approaches to modeling the wicking phenomenon mathematically. The older, more conventional method uses the Lucas–Washburn equation where the porous medium is assumed to be a bundle of aligned capillary tubes of the same radii (Lucas, 1918; Washburn, 1921). The newer method is based on Darcy's law where wicking is modeled as a single-phase flow through porous media (Pillai and Advani, 1996; Masoodi et al., 2007). Wicking is a function of the microstructure found inside porous media, the characteristics of the liquid involved, and time (Masoodi et al., 2007). The general relation between the wicking rate, the wicking time, and liquid characteristics is clearly described in both these wicking models that allow analytical results. The relation between the wicking rate and the microstructure of a porous medium is the most challenging, since the microstructure of porous media shows great variations (Bear, 1972).

Swelling is an important phenomenon that affects the wicking rate in many commercial products, such as papers, diapers, napkins, and wipes (Masoodi and Pillai, 2010; Masoodi et al., 2011). The swelling occurs due to the liquid absorption by constituent particles in plant-based porous materials such as paper and pulp when they come in contact with an organic liquid or water. Since the swelling changes the structure and molecular arrangement of the materials, it affects both the wettability and "wickability" of porous media (Kissa, 1996). In fact, the "swellability" of fibers is an important and useful property of paper for the paper industry since the

swelling leads to liquid absorption in the paper matrix, which in turn leads to liquid retention inside the porous paper. In the paper industry, this liquid holding capacity, which is related to the moisture content after a paper sheet dries, is called the water retention value (TAPPI, 1991).

1.2 Capillary Pressure

Capillary pressure is due to a partial vacuum created on top of the liquid-front in capillary tubes during the wicking process (Berg, 1993; Masoodi and Pillai, 2012). The difference in the surface energies of the dry and wet solid matrices leads to the creation of a capillary force at the liquid–solid interface, which is responsible for pulling the invading liquid into porous materials (Masoodi and Pillai, 2012). The capillary force originates from the mutual attraction of molecules in the liquid medium and the adhesion of such molecules to molecules in the solid medium; the wicking phenomenon occurs when the adhesion is greater than the mutual attraction (Berg, 1993).

According to fluid statics, when the wetting and nonwetting fluids meet, the capillary pressure, which is the difference in pressures across the interface between the two immiscible fluids, is defined as

$$p_c = p_{nw} - p_w \tag{1.1}$$

where p_{nw} is the pressure in the nonwetting fluid while p_w is the pressure in the wetting fluid. A force balance over the meniscus in a capillary tube (Figure 1.1) leads to the equation

$$p_{nw}\pi R_c^2 = p_w\pi R_c^2 + \gamma \cos\theta(2\pi R_c) \tag{1.2}$$

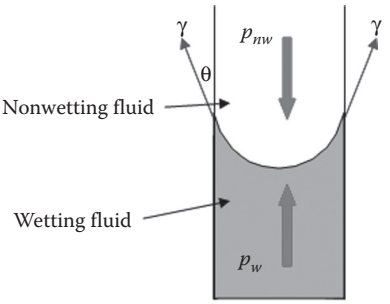

FIGURE 1.1
Meniscus (or liquid-front) in a capillary tube.

where R_c is the radius of the capillary tube. Combining Equations 1.1 and 1.2 leads to the well-known Young–Laplace equation for capillary pressure in a capillary tube:

$$p_c = \frac{2\gamma \cos\theta}{R_c} \tag{1.3}$$

Wettability is the tendency of a liquid to be attracted toward the surface of a solid phase. In a porous medium, the wettability is the main property that leads to the wicking or spontaneous imbibition (see Chapter 2). The parameter that quantifies wettability is the contact angle created by the liquid and solid phases. A lower contact angle implies a better wettability; hence, the best wettability is seen when the contact angle is zero, and the worst wettability occurs when the contact angle is 180°. (An efficient method for measuring the dynamic contact angle in porous media for a given liquid is explained in Chapter 5.)

One of the biggest challenges in using the Young–Laplace equation, Equation 1.3, is the estimation of the capillary radius. Since the real porous media with tortuous, interconnected fluid paths are not like bundles of identical, aligned capillary tubes (the "picture" used in the capillary model), some assumptions must be made to estimate the equivalent capillary radius for a real porous medium. The most accurate method of estimating the equivalent capillary radius is the capillary rise experiment, in which the upwards force due to capillary pressure is balanced by the downward force due to gravity (Dang-Vu and Hupka, 2005; Masoodi et al., 2008). The radius of the tube, employed to predict the capillary pressure given by Equation 1.3, is called the capillary radius (Masoodi et al., 2008; Masoodi and Pillai, 2012), or dry radius (Chatterjee, 1985; Chatterjee and Gupta, 2002), or static radius (Fries, 2010). The radius of the equivalent capillary tube in the wet part of the capillary tube is called the hydraulic radius (Masoodi et al., 2008; Masoodi and Pillai, 2012), wet radius (Chatterjee, 1985; Chatterjee and Gupta, 2002), or dynamic radius (Fries, 2010). Studies show that the hydraulic and capillary radii are two different variables although they are frequently used interchangeably (Chatterjee, 1985; Masoodi et al., 2008).

The analysis of micrographs of any porous medium is another way of estimating the equivalent capillary radius (Masoodi et al., 2007). Some researchers fitted circles in the pore space between particles and suggested that the circle radii should be taken as the equivalent capillary radii (Chatterjee and Gupta, 2002; Benltoufa et al., 2008). Others suggested the radius of the largest sphere (or circle, in the case of a 2-D micrograph) that could be fitted in the interparticle pore spaces should be considered the capillary radius (Lombard et al., 1989). Dodson and Sampson (1997) defined the capillary radius as the radius of a circle whose perimeter is the same as that of the pores. Masoodi and Pillai (2012) balanced the release of interfacial energy with the viscous energy dissipation at the liquid–air interface during wicking to derive the following expressions for capillary

pressure (see Chapter 5 for details) that are amenable to be used with micrographs:

$$R_c = 2\frac{A_{\text{int},s}}{C_{\text{int},s}}\frac{\varepsilon}{1-\varepsilon} \tag{1.4a}$$

$$R_c = 2\frac{A_{\text{int},v}}{C_{\text{int},v}} \tag{1.4b}$$

Here, $A_{\text{int},s}$ and $A_{\text{int},v}$ are the cross-sectional areas of solid particles and void space, respectively, at the interface; $C_{\text{int},s}$ and $C_{\text{int},v}$ are the perimeters of solid particles and void space, respectively, at the interface (note that $C_{\text{int},s} = C_{\text{int},v}$); and ε is the porosity of porous media at the interface.

Techniques also exist to measure the hydraulic radius. An indirect estimation of the hydraulic radius involves first measuring the pressure drop along a porous sample and then employing the Hagen–Poiseuille law to calculate the hydraulic radius of the imaginary capillary tubes (Dullien, 1992; Rajagopalan et al., 2001; Masoodi et al., 2008).

1.3 Examples of Wicking

Wicking occurs in nature and in everyday life. For example, wicking is responsible for transport of water and minerals in plants (Ksenzhek and Volkov, 1998). Capillarity (another name for wicking) is considered a major performance index for industrial absorbing materials, such as wipes, diapers, and commercial wicks (Chatterjee and Gupta, 2002; Masoodi et al., 2007, 2011). Figure 1.2 shows an example of wicking in toilet paper where the liquid is being pulled up by capillary pressure at the liquid-front. An example of wicking due to the combination of an external pressure and capillary pressure occurs during the wiping of a surface by a wipe, paper napkin, or sponge (Mao and Russell, 2002, 2003; Lockington and Parlange, 2003; Gane et al., 2004; Masoodi et al., 2010). In the liquid composite molding (LCM) process for making polymer composites (see Figure 1.3), the capillary pressure is imposed at the micro-fronts inside fiber bundles of a woven or stitched fabric to model delayed wetting of bundles in dual-length-scale porous media (Pillai, 2002). The capillary pressure plays an important role in the formation of voids during the LCM mold-filling process; at low capillary numbers, the wicking flow inside fiber bundles in a fabric leads to trapping of macro-voids between the fiber bundles (Pillai, 2004).

Wicking and liquid absorption are important characteristics of textile materials (Patniak et al., 2006). One of the most important applications of wicking is in the printing industry where ink has to be absorbed efficiently

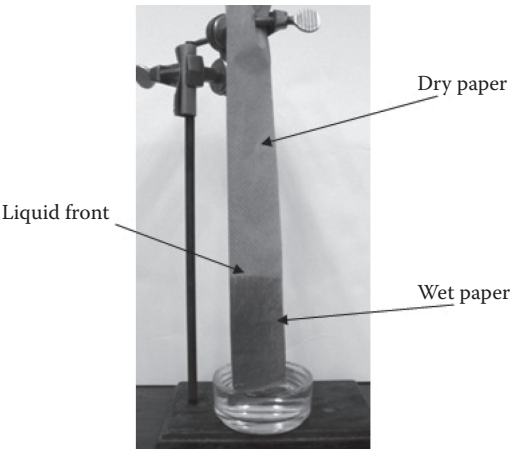

FIGURE 1.2
Wicking in toilet paper.

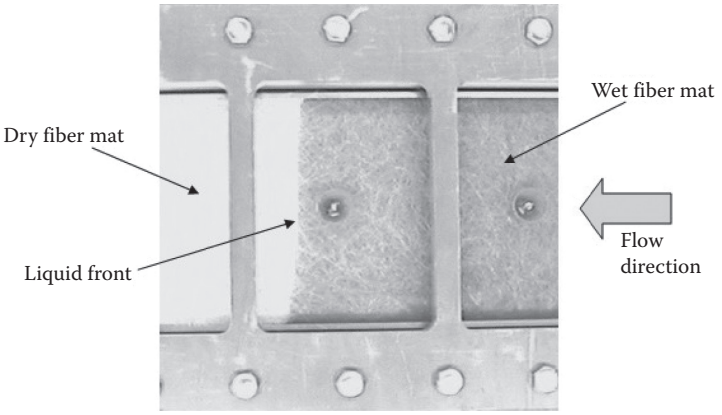

FIGURE 1.3
Injection of liquid in a mold filled with compressed fiber mats.

by paper (Gane et al., 2000; Schoelkopf et al., 2000; Schoelkopf, 2002). Using wicks made from polymers, ceramics, or textiles to dispense air fresheners or insecticides to room air is another industrial application of wicking (Masoodi et al., 2007, 2008). The astronauts use a device called spacecraft propellant management device (PMD) for movement in space, where the movement of liquid fuel through capillarity in low-gravity environments is of high importance (Fries, 2010). Heat pipes are very important in the field of microelectronic cooling (Faghri, 1995). The driving force in heat pipes is wicking or capillarity, used for moving liquid from the cold end to the hot end of the heat pipe (Figure 1.4). Researchers have made nanowick devices,

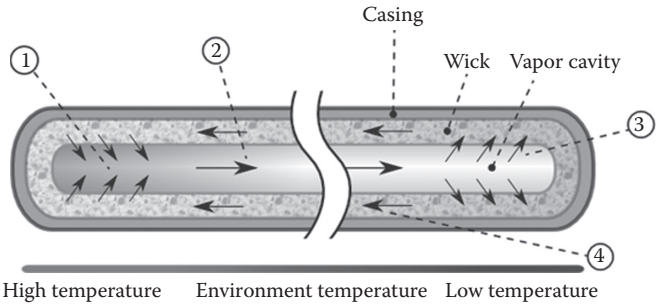

FIGURE 1.4
A schematic diagram describing fluid flow inside a heat pipe. (From Zootalures. 2006. Heat pipe mechanism, Wikipedia, The Free Encyclopedia, http://en.wikipedia.org/wiki/File:Heat_Pipe_Mechanism.png#filelinks (accessed January 4, 2012).)

using tiny copper spheres and carbon nanotubes, to passively wick a coolant toward hot electronics (Venere, 2010). Using such nanowicks, scientists have developed an advanced cooling technology for high-power electronics in military and automotive systems that is capable of handling up to 10 times the heat generated by conventional computer chips (Venere, 2010).

1.4 Modeling of Wicking in Porous Materials

There are several approaches to modeling the wicking process in porous media. To model wicking or spontaneous imbibition in a porous medium, a mathematical theory is needed to predict the all-important wicking speed in terms of the capillary pressure and the characteristics of the porous medium and the invading liquid. The following modeling approaches for wicking in porous substrates and incorporating different mathematical theories are introduced in the forthcoming chapters.

1.4.1 Wicking Models Based on the Capillary Model

In some of the traditional wicking models, the porous medium is modeled as a bundle of aligned capillary tubes. The first mathematical theory of capillary rise in a tube was published by Lucas (1918) and Washburn (1921) independently. They used momentum balance and neglected gravity and inertial

effects to derive an analytical solution for meniscus height as a function of time in a vertical capillary tube. The capillary force was balanced with the viscous force in the tube to arrive at the well-known Lucas–Washburn equation. Later, others tried to include the neglected or missed force terms in the momentum equation and improved the accuracy of the capillary model (Chapter 3). In a recent development, the fractal theory was employed to include the statistical information about porous media in order to improve the accuracy of the capillary model for complex and irregular geometries (Chapter 10).

1.4.2 Porous-Continuum Models

Under the porous-continuum models, the flow in a porous medium is typically averaged over an averaging volume much larger than the individual pores or particles/fibers, but much smaller than the overall size of the medium. Thus, the averaged flow-variables are employed to predict flows in porous media after incorporating the properties of the liquid and solid phases through averaged medium properties (Chapter 4). The governing equations for wicking flows under isothermal conditions are Darcy's law and the continuity equation. Darcy's law is an empirical formula published in 1856 by Henry Darcy based on the results of his experiments on the flow of water through beds of sand (Bear, 1972). There are two general approaches to model fluid flow using the porous-continuum models: (1) the single-phase flow approach and (2) the two-phase flow approach. In the single-phase flow approach, a clearly defined liquid-front in a porous medium is postulated behind which the pore space is assumed to be completely occupied by the invading liquid.* Such a model has been used for modeling wicking in both rigid and swelling porous media (Chapter 5). In the two-phase flow approach, both the wetting and nonwetting fluids are modeled using Darcy's law, which leads to Richards' equation for predicting saturation migration in partially saturated porous media (Chapters 4 through 6). Hence, Richards' equation has been employed frequently to model wicking in rigid porous media (Chapters 4 through 6), and in nonrigid, swelling porous media (Chapter 7). The mixture theory can also be used to set up the averaged governing equations for flow in a deforming porous media (Chapter 11).

1.4.3 Discrete Models

One prominent example of the discrete models is the pore network model that uses pore-level physics to simulate fluid motion and transport within porous media. The geometry of such a pore network is designed to represent the structure of a real porous medium through a "reconstruction" process. The pore network is modeled as a network of pores (also called nodes) that are interconnected to each other through throats (also called bonds). The

* See some examples of sharp liquid-fronts in Figures 1.2 and 1.3.

modeling approach can be either single-phase or two-phase depending on whether just the liquid phase is being considered or both the liquid and gas phases are being considered within the pore space of the network in the mathematical model (Chapters 8 and 9).

1.4.4 Statistical Models

In statistical models, the statistical information about the microstructure of a porous medium is used to determine variability in the macroscopic (or porous-continuum) properties of a porous medium. The Lattice–Boltzmann method (LBM) is an approach based on statistical mechanics for modeling wicking in porous media. In LBM, instead of solving the Navier–Stokes equations, the discrete Boltzmann equation is solved to simulate the flow of multiple fluids within the complicated pore geometries (Chapter 12).

1.5 Summary

Wicking or spontaneous imbibition is a very common natural phenomenon where a liquid moves spontaneously into dry porous materials due to the release of surface energies. For example, the transportation of water and minerals from roots to the upper parts (leaves and branches) of trees involves wicking. Wicking is also very important in many consumer products, including wipes, diapers, feminine pads, and dispensers of insecticides and air fresheners. Wicking also has important industrial applications, such as heat pipes and nano-wicks, which are used for cooling microelectronic devices. This chapter introduces the capillary (suction) pressure, the main cause of the wicking phenomenon. The different available approaches for the estimation of the capillary and hydraulic radii, the two important wicking parameters, are explained. Finally, an overview of different modeling approaches for wicking is provided where the traditional capillary models, the porous-continuum models, the discrete models, and the statistics-based models are introduced; these models will be explored in greater detail in Chapters 3 through 12.

Nomenclature

Roman Letters

A	Area (m^2)
C	Perimeter (m)

p	Pressure (Pa)
R	Radius (m)

Greek Letters

θ	Contact angle (degree)
γ	Surface tension (N/m^2)
ε	Porosity (dimensionless)

Subscripts

c	Capillary
int	Interface surface of dry and wet matrix
nw	Nonwetting
s	Solid
v	Void space
w	Wetting

References

Alava, M., Dubé, M., and Rost, R. 2004. Imbibition in disordered media. *Advances in Physics* 53: 83–175.

Bear, J. 1972. *Dynamics of Fluids in Porous Media*. New York, Elsevier Science.

Benltoufa, S., Fayala, F., and BenNasrallah, S. 2008. Capillary rise in macro and micro pores of Jersey knitting structure. *Journal of Engineered Fibers and Fabrics* 3(3): 47–54.

Berg, J.C. 1993. *Wettability*. New York, Marcel Dekker.

Chatterjee, P.K. and Gupta, B.S. 2002. *Absorbent Technology*. Amsterdam, Elsevier.

Chatterjee, P.K. 1985. *Absorbency*, Amsterdam/New York, Elsevier.

Dullien, F.A.L. 1992. *Porous Media: Fluid Transport and Pore Structure*. San Diego, Academic Press.

Dodson, C.T.J. and Sampson, W.W. 1997. Modeling a class of stochastic porous media. *Applied Mathematics Letters* 10(2): 87–89.

Dang-Vu, T. and Hupka, J. 2005. Characterization of porous materials by capillary rise method. *Physicochemical Problems of Mineral Processing* 39: 47–65.

Fries, N. 2010. *Capillary Transport Processes in Porous Materials—Experiment and Model*. Göttingen, CuvillierVerlag.

Faghri, A. 1995. *Heat Pipe Science and Technology*. New York, Taylor & Francis Group.

Gane, P.A.C., Ridgway, C.J., and Schoelkopf, J. 2004. Absorption rate and volume dependency on the complexity of porous network structures. *Transport in Porous Media* 54: 79–106.

Gane, P.A.C., Schoelkopf, J., Spielmann, D.C., Matthews, G.P., and Ridgway, C.J. 2000. Fluid transport into porous coating structures: Some novel findings. *Tappi Journal* 83: 77.

Ksenzhek, O.S. and Volkov, A.G. 1998. *Plant Energetics*. San Diego, Academic Press. 1st edition.

Kissa, E. 1996. Wetting and wicking. *Textile Research Journal* 66(10): 660–668.

Lockington, D.A. and Parlange, J.Y. 2003. Anomalous water absorption in porous materials. *Journal of Physics D: Applied Physics* 36: 760–767.

Lucas, R. 1918. Rate of capillary ascension of liquids. *Kollid Z* 23: 15–22.

Lombard, G., Rollin, A., and Wolff, C. 1989. Theoretical and experimental opening sizes of heat-bonded geotextiles. *Textile Research Journal* 59(4): 208–217.

Masoodi, R. and Pillai, K.M. 2010. Darcy's law-based model for wicking in paper-like swelling porous media, *AIChE Journal* 56(9): 2257–2267.

Masoodi, R. and Pillai, K.M. 2012. A general formula for capillary suction pressure in porous media. *Journal of Porous Media* 15(8): 775–783.

Masoodi, R., Pillai, K.M., and Varanasi, P.P. 2007. Darcy's law based models for liquid absorption in polymer wicks. *AIChE Journal* 53(11): 2769–2782.

Masoodi, R., Pillai K.M., and Varanasi P.P. 2008. Role of hydraulic and capillary radii in improving the effectiveness of capillary model in wicking. *ASME Summer Conference*, Jacksonville, FL, USA, August 10–14.

Masoodi, R., Pillai, K.M., and Varanasi, P.P. 2010. The effect of hydraulic pressure on the wicking rate into the wipes. *Journal of Engineered Fibers and Fabrics* 5(3): 49–66.

Masoodi, R., Tan, H., and Pillai, K.M. 2011. Numerical simulation of liquid absorption in paper-like swelling porous media. *AIChE Journal*. DOI 10.1002/aic.12759.

Mao, M. and Russell, S.J. 2002. Prediction of liquid absorption in homogeneous three dimensional nonwoven structures. *International Nonwoven Technological Conference*, Atlanta.

Mao, N. and Russell, S.J. 2003. Anisotropic liquid absorption in homogeneous two dimensional nonwoven structures. *Journal of Applied Physics* 94(6): 4135–4138.

Pillai, K.M. 2002. Governing equations for unsaturated flow in woven fiber mats: Part 1 Isothermal flows. *Composites Part A: Applied Science and Manufacturing* 33:1007–1019.

Pillai, K.M. 2004. Unsaturated flow in liquid composite molding processes: A review and some thoughts. *Journal of Composite Materials* 38(23): 2097–2118.

Pillai, K.M. and Advani, S.G. 1996. Wicking across a fiber-bank. *Journal of Colloid and Interface Science* 183: 100–110.

Patniak, A., Rengasamy, R.S., Kothari, V.K., and Ghosh, A. 2006. Wetting and wicking in fibrous materials. *Textile Progress Woodhead* 38(1): 1–105.

Rajagopalan, D., Aneja, A.P., and Marchal, J.M. 2001. Modeling capillary flow in complex geometries. *Textile Research Journal* 71(91): 813–821.

Schoelkopf, J. 2002. Observation and modelling of fluid transport into porous paper coating structures. Ph.D. Thesis, University of Plymouth, U.K.

Schoelkopf, J., Gane, P.A.C., Ridgway, C.J., and Matthews, G.P. 2000. Influence of inertia on liquid absorption into paper coating structures. *Nordic Pulp Paper Research Journal* 15: 422.

Sorbie, K.S., Wu, Y.Z., and McDougall, S.R. 1995. The extended washburn equation and its application to the oil/water pore doublet problem. *Journal of Colloid Interface Science* 174: 289.

TAPPI Useful Methods. 1991. *Water Retention Value (WRV), UM-254, 54-56.* Atlanta, TAPPI Press.

Venere, V. 2010. Nanowick at heart of new system to cool power electronics. http://www.eurekalert.org/pub_releases/2010–07/pu-nah072210.php.

Washburn, E.V. 1921. The dynamics of capillary flow. *Physical Review* 17: 273–283.
Zootalures. 2006. Heat pipe mechanism, Wikipedia, The Free Encyclopedia, http://en.wikipedia.org/wiki/File:Heat_Pipe_Mechanism.png#filelinks (accessed January 4, 2012).

2

Wettability and Its Role in Wicking

Jijie Zhou

CONTENTS

Wicking plays a significant role in many separation processes, for example, chromatography. Porous and fabric networks can guide small amounts of liquid flow with wetting and spreading forces, and are themselves treated by chemicals in the liquid solution in the meantime. The first impression on such a spontaneous liquid-delivery process is often analogous to a capillary rise in small tubes. Similar to the chemical potential, liquids tend to minimize the summation of interfacial energies by changing their shapes. In this chapter, we interpret the deformable interfaces between immiscible fluids in terms of wetting parameters, such as surface energy, spreading parameter, and contact angle. Various concepts are brought in and connected to an illustrative and relevant role in wicking. A generalized view in film transport and hydrodynamics is outlined, and measurement methods for wetting parameters are listed.

2.1 Introduction

Wicking is referred to as the action of the spreading of a liquid through a textile network with capillary-like motions. The process of wicking involves physical

chemistry of a surface, liquid properties, concave menisci, interfacial topography, ambient, and operating conditions. Application of basic sciences and engineering principles to the development, design, and operation of the process may control wicking toward a more valuable form; engineering improvement involves more intrinsic material designs than auxiliary instrumentation.

In the early nineteenth century, an English physician, Thomas Young, observed the liquid contact angle on a ridge surface and discovered the phenomena of capillary action on the principle of surface tension; a French scientist, Simon-Pierre Laplace, discovered the significance of meniscus radii with respect to capillary action. These discoveries led to the hydrostatic Young–Laplace pressure (ΔP) at a curved interface as a landmark of the field, where the pressure difference traversing the boundary is proportional to the mean curvature, that is, the average of two principle radii of curvature at the interface (or average of the maximum κ_1 and minimum κ_2 curvature values of this interface). The Young–Laplace pressure can explain shape factors such as the reason for small bubbles to merge themselves into connected large ones.

Surface-active agents (surfactants) practically act as detergents, wetting agents, emulsifiers, foaming agents, and dispersants. The effects of surfactants on wetting are a direct evidence of the intermolecular nature of a wetting force. The Marangoni effect, named after an Italian physicist, accumulates solvent molecules in opposition to the surfactant concentration gradient. Owing to concentration or temperature variations, liquid is conveyed along the consequential surface tension gradient to accommodate the Marangoni traction, to advance the liquid front, and to enlarge the wetted surface area (namely, to spread).

As an interfacial nature, surfaces carry a specific energy (surface energies) named surface tension. This energy reflects the cohesion of the condensed phase. Its quantity, from Zisman's empirical criterion, predicts wetting performance. Interfacial morphologies and energies coexist as we model wettability, capillarity, and related phenomena; in addition, the meniscus structure at the liquid advancing front counts as well as density, concentration, and pressure.

Wetting parameters play a fundamental role in wicking, similar to the Navier–Stokes equations with respect to turbulence. Hierarchical structures account for most complexity. Since 2000, the Clay Mathematics Institute has offered a million-dollar prize to the conjectures of existence and smoothness of the Navier–Stokes solutions. Wicking, or specifically imbibition, possesses complicated boundary conditions, absorbent mechanisms, and consequentially different assumptions in different models.

2.2 Wetting and Its Intermolecular Origin

Soap, a premier surfactant, was produced in 600 BC from tallow and beech ashes by the Phoenicians. The amphiphilic nature of soap molecules makes

them to invade an immiscible water–oil interface, so that they become the compound of detergents and the main component of biological membranes. Modification of interfacial structures increases the affinity of water molecules to the interface. The degree of wetting or wettability is determined by intermolecular interactions when two materials are brought together, or when a liquid solution comes into contact with matter. Molecular rearrangements at interfaces lead to surface-state changes. The surface composition changes at a much faster rate than the bulk population. For instance, the interface quickly becomes more solute-rich than the solution.

A water wettable surface is termed hydrophilic; otherwise hydrophobic. Hydrophilic and lipophilic concepts are extended to interaction between molecules as well. Since disrupting the existing water structure at hydrogen-bonding sites is entropically unfavorable, water molecules barely reorient or restructure themselves around nonpolar solute or hydrophobic surfaces. As a consequence, nonpolar solute molecules deform their size and shape to become accommodated in an aqueous medium, which results in the hydrophobic effect. When a transition to wetting occurs, for entropic reasons, the liquid surface tension is so small that the free energy cost in forming a thick film is sufficiently compensated by liquid–solid interaction.

There are two theoretical approaches to formulate the foundation of wetting: the equation of state approach and Lifshitz–van der Waals/acid-base (LW/AB) approach. The first one assumes that an equation of state-type relation exists and employs the Gibbs–Duhem equations at interfaces; the other sums all attraction forces bearing on the surface molecules. Both exist as an immediate consequence of hypotheses and breaks down upon experimental checks of internal consistency. For example, surface energies are calculated on the continuum basis of the Lifshitz theory, or in terms of pairwise additivity of individual atoms or molecules. The theoretical surface energies $\gamma \approx A/24\pi(0.165\ \text{nm})^2$, where A is the Hamaker constant, are in good agreement with the experimental measurements for a variety of liquids and solids, except for strong hydrogen-bonding liquids where H-bonded network is nonpairwise additive. Perturbation of the hydrogen-bonding network is the origin for the enhancement of excess surface free energy.

Intermolecular and surface forces typically involve van der Waals, electrostatic, steric, depletion, hydrophobic, and salvation interactions. They are either essentially electromagnetic or steric in origin. In some cases, oscillatory period and fluctuation account for these forces; aggregation often raises geometric packing considerations due to solute concentration. The strength and decay length of each interaction characterize its force. The average translational kinetic of a molecule is $\frac{3}{2}\,kT$. Thermal energy kT is used to gauge the strength of an interaction.

As an ambiguous intermolecular force, van der Waals interaction is essentially electrostatic; it is a weak charge-fluctuation force that gradually dies away as the sixth power of molecular separation, which is very small when compared with the thermal energy kT. It may sometimes loosely refer to all

intermolecular forces. The van der Waal's equation of state was first derived in 1873, assuming that a fluid composed of particles that occupy a finite volume and exert forces on each other. Taking these effects into account, the van der Waal's equation of state is cast into the form:

$$\left(P + \frac{a}{V^2}\right)(V - b) = n \cdot RT \tag{2.1}$$

where $R = 8.3143$ J mol^{-1} K^{-1} is the universal gas constant. The interaction decays so fast that the sum of interactions between the molecules is considered two at a time, without significant influence of other nearby molecules. Van der Waals interaction defines the chemical character of many organic compounds. The typical surface tension of a van der Waals liquid or solid is $\gamma = 33$ mJ m^{-2}.

To elucidate the interplay between intermolecular and surface forces and the resulting wetting properties of a liquid, molecular dynamics (MD) simulations have been employed to understand liquid behaviors confined in a nano-scaled system. Despite its intermolecular origin, wetting is a macroscopic observation with many characteristic parameters to describe its physics and phenomena. Surface tension is equivalently a binary interfacial tension, suspending along a few molecular layers, where molecules attract each other the most. Surface tension is a well-defined material property on an atomically smooth and chemically homogeneous surface, when its value is irrelevant to a change in thickness. The hydrostatic Young–Laplace pressure (ΔP) traversing a curved membrane is proportional to the surface tension (γ) of the membrane which leads to

$$\Delta P = \gamma(\kappa_1 + \kappa_2) \tag{2.2}$$

where κ_1 and κ_2 are principle curvatures of the membrane (Figure 2.1).

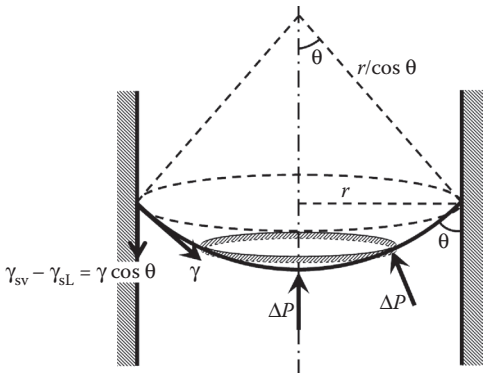

FIGURE 2.1
Liquid rise in a capillary.

2.2.1 Heuristic Derivation: How a Partial Wetting Liquid Rises into a Capillary with Wetting Parameters

When the partial wetting liquid comes into contact with the inner surface of the capillary, the immersed inner surface witnesses a solid–liquid interfacial energy (γ_{sL}) smaller than before (solid–vapor, γ_{sv}). This gives the liquid an advancing force $2\pi r(\gamma_{sv}-\gamma_{sL})$ to wet more capillaries. The advancing force is initially balanced with liquid momentum. As the liquid rises higher into the capillary, the viscous drag as well as gravity, slows down the liquid. Statically, the liquid reaches its balance when the deformable interface adapts Young's relation

$$\gamma \cos\theta = \gamma_{sv} - \gamma_{sL} \tag{2.3}$$

at the triple line, and when gravity nullifies the effect of Laplace pressure (ΔP) that originates from the liquid–vapor interfacial energy (γ). With θ angle at the circular triple line, the liquid–vapor interface has to conform into a bowl shape. Pressure along the vapor side of the interface is the same everywhere as the ambient pressure; transverse pressure is induced by radii of curvature. By neglecting the weight of the liquid in the depth of the bowl shape, transverse pressure will become constant on the interface. Consequently, the radii of curvature in the Laplace pressure formula $\Delta P = \gamma(\kappa_1 + \kappa_2)$ become a constant. Applying the triple-line boundary condition of θ, we obtain $\kappa_1 = \kappa_2 = \cos\theta/r$.

2.3 Contact Angle and Triple Line

Contact angle of a liquid to a substrate is the geometrical angle of a liquid/vapor interface meeting a solid surface, which is formed at the three-phase boundary. It is a quantitative measure of wetting affinity. The line of contact where three phases intersect is termed triple line or contact line when advancing.

Contact angle (θ) of one liquid has a narrow value of measurement on an ideal, flat, homogeneous, ridged surface, for example, on a semiconductor silicon wafer. Contact angle of mercury with glass is about 140°. Realistically, the contact angle on a rough surface may vary by 30° or 40°. Upon volume change, a liquid droplet may maintain its root area on the substrate invariant by adjusting its height and contact angle. Such an observation of pinning established hysteresis mechanisms of the triple line. While the triple line is pinned, the contact angle exists between two limiting values—advancing contact angle (θ_a) and receding contact angle (θ_r), which are the maximum and minimum values, respectively. Beyond these values, the line of contact moves.

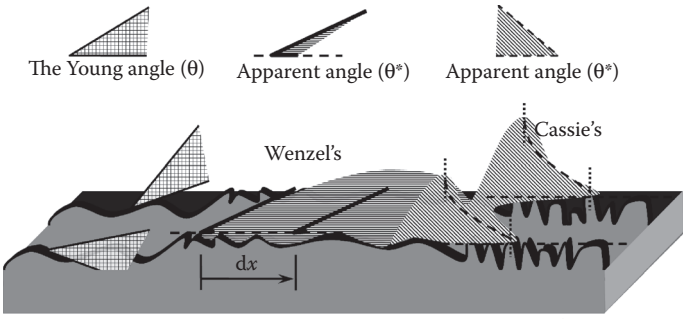

FIGURE 2.2
Apparent contact angles.

The liquid, as described by Shuttleworth and Bailey (1948), leaves a bit of "wonder" in its wake, that is, the receding contact angle may not have a unique value. Experimental range of observable contact angles, that is, the measurable and reproducible values of the contact angle, is in between the advancing and the receding contact angles. There is another contact angle, associated with the thermodynamic equilibrium configuration of the three-phase boundary/intersection system. This equilibrium contact angle is coupled with a global energy minimum, sometimes named as the Young angle linked to solid surface energies, and commonly referred to as the contact angle.

Contact angle on a chemically heterogeneous surface (a mixture of θ_1 and θ_2 with f_1 and f_2 representing the fractional surface areas) is studied in Cassie and Baxter (1944) relation

$$\cos\theta^* = f_1 \cos\theta_1 + f_2 \cos\theta_2 \tag{2.4}$$

The apparent angle (θ^*) is restricted between θ_1 and θ_2. Particularly, if the heterogeneous surface consists of air, that is, the liquid is lifted up by air pockets on roughness features, the apparent contact angle (θ^*) on this composite surface can be written as

$$\cos\theta^* = \varphi_s \cos\theta - (1 - \varphi_s) \tag{2.5}$$

where φ_s is the pillar density on the solid surface. The defects and contaminants make many values of the contact angle possible, and thus leading to pinning of the triple line (Figure 2.2).

2.3.1 Roughness

Similar to a chemically heterogeneous surface, the apparent contact angle is modified on a rough-textured surface. Influence of geometric roughness

(*r*: ratio of a rough surface area to a smooth planar one) on the contact angle was first explained by the Wenzel (1936) model via counting in the surface energy over the whole rough surface area. Wenzel's relation gives

$$\cos\,\theta^* = r\cos\theta \tag{2.6}$$

Since roughness $r > 1$, it does not alter nonwetting into a wetting surface, but makes the hydrophilic surface more hydrophilic and the hydrophobic surface more hydrophobic. Besides following contours of the rough surface as in Wenzel's relation, the liquid may suspend a composite surface of the solid material and air pockets (Cassie and Baxter relation). Owing to the small solid–liquid contact area in the Cassie and Baxter state, the hysteresis is small and a liquid drop may roll off easily. The nematic arrangement seen in rice leaves, leads to anisotropic wetting; high base radii and rounded protrusions in roughness design, as seen in lotus leaves, are advantageous to self-cleaning and superhydrophobicity.

On a rough surface, as illustrated by He et al. (2003), two distinct apparent contact angles are possible in terms of reaching the local stable energy state, modeled by either Cassie's or Wenzel's theory, although one has a global lower energy than the other local minimum; that is associated to the thermodynamic equilibrium configuration, liquid meniscus on rough surfaces can be in the bi-stable Wenzel/Cassie state, depending on the initial location of a droplet. Furthermore, the influence of roughness on the contact angle is asymmetric when comparing hydrophilic ($\cos\theta > 0$) with hydrophobic ($\cos\theta < 0$) wetting. From partial wetting to complete wetting, Wenzel's model ceases to be applicable as $\cos\theta$ approaches 1; from hydrophobic to nonwetting, roughness dramatically alters hydrophobicity into superhydrophobicity. Such observations often involve the coexistence of two scales of roughness or random roughness. Shibuichi et al. (1996) have demonstrated that hierarchical roughness enables plant surfaces not only to reach a very high degree of hydrophobicity (i.e., $\cos\theta$ close to –1), but also a low contact angle hysteresis (i.e., a small difference between the advancing and receding angle). On the other, ideal substrates with an atomically smooth surface, for example, semiconductor silicon wafers, elastomers cross-linked from a liquid film, and the Pilkington floated glass are investigated to diminish the hysteresis ($\Delta\theta = \theta_a - \theta_r$). The difference between the advancing and receding angle reflects the change in the moisture content of the substrate—as a liquid drop is about to advance, the liquid sees a rough dry solid beyond the drop; when the liquid recedes, it leaves a trail of a mixture of solid and liquid at its wake. Consequential imbibition and drainage, in lieu of wetting, are still under investigation. Pinning of a contact line on either chemical heterogeneities or roughness incorporates nonlinearity into wicking, is similar to evaluating contributions from a dynamic load or a static friction. Since neither roughness nor fractional surface area is a continuum variable, applying them into wicking becomes a model-sensitive approach.

The maximal "chemical hydrophobicity" for water is 120°. Although hierarchical roughness promotes superhydrophobicity, the involved roughness is in the order of micrometers and submicrons. However, several chromatographic wicking studies involve nanometer-sized interstices.

2.3.2 Fine Structure of the Triple Line

Exquisite surface structures have been fabricated to study both beneficial and unfavorable effects of roughness on wetting. At pinning sites where the contact line is jammed before it suddenly jumps, the local curvature makes a range of contact angle accessible at that neighborhood, and that range allows a drop to deform against an external force and to cling on a surface. Microscopically, the contact line pinned at a single nonuniform spot adopts a characteristic saddle shape. Such fine structures are studied for the advancing front of hemi-wicking. The triple line is an averaged observation on a macroscopic level. The validity of the Wenzel model is restricted to such large drops that projection of a single defect is evened out.

The contact angle becomes size dependent in the nano regime, for example, water contact angle on carbon nanotubes. Line tension on small drops becomes an additional force to the contact angle θ that is given in Young's relation $\gamma \cos \theta = \gamma_{sv} - \gamma_{sL}$. At the molecular level, the definition of triple line is practically not the merging line as liquid thickness changes to zero, for example, tetrasiloxane meets the solid in layers resembling an inclined wavy slope. For small wetting molecules, there are also visible deformations on the Young angle; there exists a point of inflection in the immediate vicinity of the triple line. Such relevant spatial observations are typically a few to tens of nanometers. When the surface roughness is not in a regular pattern, it is hard to incorporate the geometry factors into consideration on the surface with nanotopographies, not only because of the difficulty of fabrication, but also because of the lack of dedicated work on superhydrophilic surfaces. In an effort of modeling macroscopically observed viscous dynamics on nanotextured surfaces, theoretical understanding often assumes that the effect of pinning and depinning from each nanopillar is not important.

A particular note is that contact angle in dynamic wetting is speed-dependent because the dynamic contact angle contributes to the formation of newly wetted solid surface. When a liquid sheet impinges onto a moving solid substrate, the actual contact angle depends not only on the wetting speed and material properties of the contacting media, but also on the inlet velocity of the liquid and geometry near the moving contact line. In complete wetting regime, a velocity-dependent dynamic contact angle

$$\theta \propto \nu^{1/3} \tag{2.7}$$

gives the relationship between θ and the speed of spreading (ν).

2.4 Interfacial Tension and Spreading Parameter

Interfacial width between immiscible polymer phases is in the order of 1–3 nm, where one polymer protrudes into the other domain by a random walk of its loop. The interfaces for small molecules are typically a few atomic layers thick, where surface atoms are not in the same arrangement as in the bulk. On an ideal case in solids, the so-called singular surface, each asymmetrically located atom moves toward the interior, which results in an appreciable reduction of lattice constant between the surface atoms and interior atoms. Such a perpendicular shift of the surface layer may accompany lateral shift or restructuring of the original lattice. It is common that pure material surfaces reduce its surface energy by chemical and physical adsorption. Particularly, enrichment of surfactants on the surface of a liquid effectively reduces the surface energy. Liquid molecules on a liquid–vapor interface are prone to maintain a greater space than those inside the bulk and as a result interfacial molecules experience more attractive force than the interior ones. In contrast to solids, molecule lattice or spatial pattern on liquid surface seldom shifts, reconstructs or shrinks. The liquid surface acts as a stretched membrane, characterized by a surface tension (or interfacial tension) that opposes its distortion.

As liquid deforms continuously when subjected to shear stress, capillary adhesion and stable shapes of dew is a consequence of surface tension. Surface tension is also the physical origin of capillarity and wetting phenomena. Surface tension can be viewed as energy per unit area, which is numerically similar to the surface free energy required for generating more surface or surface area. Surface energy of simple liquids and solids in their own vapor is determined by the material property of a substance. In a foreign vapor, the process of creating surface area results in lowering the value of surface energy. While supplying energy to create a surface, the work required is proportional to the number of molecules on the new surface area, that is, $dW = \gamma\, dA$. If cohesion energy inside a liquid is U per molecule, the molecules missing half of the neighbors on the surface find themselves short of $U/2$. If Θ^2 is roughly each molecular exposed area, the surface tension of this liquid becomes $U/2\Theta^2$. The intensity of surface free energy is driven by the density of atomic dislocation and defects rather than their precise arrangement.

When the amount of liquid in a sessile drop exceeds its advancing contact angle, the triple line moves and this can be explained in both energy and force angle of view. The surface free energy can be viewed as surface tension, a force per unit length, directed toward the liquid along the local radius of curvature on any intersected curve, that is, $dF = \gamma\, dL$, or $d\sigma = \gamma\, dx$. The rate at which the rim of the drop advances over the solid surface is determined by the influence of gravity viscosity and capillarity, the volume of liquid in the drop, the contact angle, and the slip at the contact line.

In the field of materials science, surface tension is also referred to as surface stress, interfacial free energy, or surface free energy. The liquid sees a substrate (or another immiscible liquid) as one of the three types of wetting, that is, there are three types of behaviors of a liquid drop with its substrate: (i) complete wetting, (ii) partial wetting, and (iii) partial nonwetting. Lenient usage of the term "wetting" is also applied to the substance other than water. These behaviors are characterized by spreading the parameter and contact angle. By force balance of surface stress at the triple line (or alternatively from surface-free-energy point of view, work done to displace the contact line), contact angle θ is given in Young's relation: $\gamma \cos\theta = \gamma_{sv} - \gamma_{sL}$. Spreading parameter ($S$) is defined as

$$S = \gamma_{sv} - \gamma_{sL} - \gamma \tag{2.8}$$

The three types of wetting correspond to sign changes: (i) $S > 0$ and $\theta = 0$—complete wetting, (ii) $S < 0$ and $\theta < 90°$—partial wetting, and (iii) $S > 90°$—partial nonwetting (Figure 2.3).

Disjoining pressure of a film is a repulsive pressure analogous to the repulsive van der Waals force across the adsorbed liquid film. It only becomes significant when the film is very thin, that is, thinner than 100 nm and it causes the liquid to spread on surfaces. When liquid is pure water, electrically charged layers spontaneously form at both liquid–gas and solid–liquid interfaces; such charged layers and their electrostatic interaction are typical within a range of 10 nm. The water surface could be slightly deformed, which allows it to relax the additional stress from confinement and artificial boundary. Disjoining pressure is rather long range, varying as $1/e^3$. For example, a film of thickness e and surface tension γ is placed on a solid wafer whose surface tension is γ_{sv} and γ_{sL}. As liquid thickness vanishes on the substrate, the energy of the bare solid is recovered, that is,

$$\gamma_{sv} = \lim_{e \to 0} \gamma_{sL} + \gamma + \varphi(e) \tag{2.9}$$

Therefore, when the film thickness tends to zero, $\varphi(e, e = 0) = \gamma_{sv} - \gamma_{sL} - \gamma = S$; when the film thickness tends to large $\varphi(e, e = \infty) = 0$. This corrective term

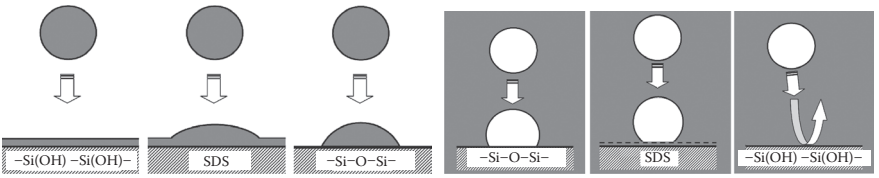

FIGURE 2.3
Wetting and nonwetting on a chemically modified surface.

$\varphi(e)$ is associated with the interfacial energies and one of formulations for the disjoining pressure produced by the two interfaces of the liquid film is

$$p(e) = -d\varphi/de > 0 \tag{2.10}$$

Disjoining pressure is related to the chemical potential $\mu = \mu_o - v_o\, p(e)$; if the film thickness is changed by adding molecules $dN = de/v_o$, change of the energy includes

$$M\,dN = \mu_o\, dN + p(e)\, de \tag{2.11}$$

Disjoining pressure is also a combination of various physical forces, that is, molecular, electrostatic, and structural; when the presence of intermolecular interactions is summarized into the disjoining pressure, the effective interface potential becomes the cost of free energy to maintain a homogeneous wetting film of thickness e. In case of partial wetting, for example, as described by Derjaguin and Kussakov (1939), the capillary pressure produced by meniscus at curved interfaces is in equilibrium with the connected disjoining pressure produced by the liquid-adsorbed layer.

These two aspects—energy and force—are typical approaches to study surface (interfacial) tension. The Young–Laplace pressure can explain capillary bridges, as a lateral cohesive force to consort the dissolved particles into clusters, or to maintain wet hairs adhering to bundles. Surface-to-volume ratio is a typical parameter in wicking studies. In hydrodynamic or dynamic studies, interfacial tension is also referred to as tension or wetting tension (τ) (Figure 2.4).

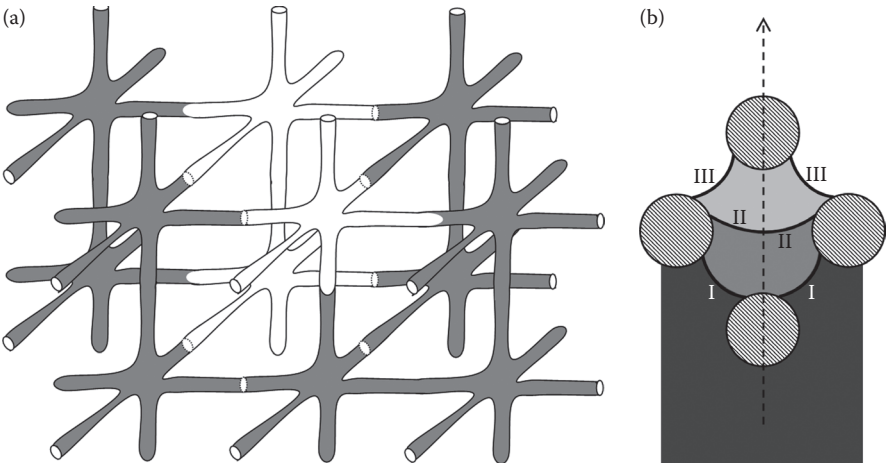

FIGURE 2.4
Wicking into porous network. (a) Partial filling of connected narrow pores; (b) sequential menisci while liquid passing obstacles in time course.